The Role of Gly-4 of Human Cystatin A (Stefin A) in the Binding of Target Proteinases. Characterization by Kinetic and Equilibrium Methods of the Interactions of Cystatin A Gly-4 Mutants with Papain, Cathepsin B, and Cathepsin L[†]

Sergio Estrada,[‡] Maria Nycander,[‡] Nikki J. Hill,[§] C. Jeremy Craven,[§] Jonathan P. Waltho,[§] and Ingemar Björk*,[‡]

Department of Veterinary Medical Chemistry, Swedish University of Agricultural Sciences, Uppsala Biomedical Center, Box 575, SE-751 23 Uppsala, Sweden, and Krebs Institute, Department of Molecular Biology and Biotechnology, University of Sheffield, Firth Court, Western Bank, Sheffield S10 2TN, United Kingdom

Received January 5, 1998; Revised Manuscript Received March 10, 1998

ABSTRACT: The importance of the evolutionarily conserved Gly-4 residue for the affinity and kinetics of interaction of cystatin A with several cysteine proteinases was assessed by site-directed mutagenesis. Even the smallest replacement, by Ala, resulted in ∼1000-, ∼10- and ∼6000-fold decreased affinities for papain, cathepsin L, and cathepsin B, respectively. Substitution by Ser gave further 3−8-fold reductions in affinity, whereas the largest decreases, $>10^5$-fold, were observed for mutations to Arg and Glu. The kinetics of inhibition of papain by the mutants with small side chains, Ala and Ser, were compatible with a one-step bimolecular reaction similar to that with wild-type cystatin A. The decreased affinities of these mutants for papain and cathepsin L were due exclusively to increased dissociation rate contants, but the reduced affinities for cathepsin B were due also to decreased association rate constants. The latter finding indicates that the intact N-terminal region serves as a guide directing cystatin A to the active site of cathepsin B, as has been proposed for cystatin C. The kinetics of binding of the mutants with charged side chains, Arg and Glu, to papain were consistent with a two-step binding mechanism, in which the mutant side chains are accommodated in the complex by a conformational change. The NMR solution structure of the Ala and Trp mutants showed only minor changes compared with wild-type cystatin A, indicating that the large reductions in affinity for proteinases are not due to altered structures of the mutants. Instead, a side chain larger than a hydrogen atom at position 4 affects the interaction with the proteinase most likely by interfering with the binding of the N-terminal region.

Human cystatin A (stefin A) is a cysteine proteinase inhibitor belonging to the cystatin superfamily. Cystatins are classified in three main groups. Inhibitors of family I (also called stefins), to which cystatin A belongs, consist of about 100 amino acids and have no disulfide bonds (*1*). Family II cystatins, represented by cystatin C and chicken cystatin, have about 120 amino acids and contain two disulfide bonds (*1*, *2*). Family III cystatins, or kininogens, are larger multifunctional glycoproteins, present in blood plasma, containing three family II-like domains, two of which can inhibit proteinases (*1*, *3*). Cystatins are thought to participate in the protection against unwanted proteolysis, either from endogenous lysosomal cysteine proteinases (*1*) or from proteinases released by metastasizing cancer cells (*4*) or invading microorganisms (*5*, *6*). Evidence for specific physiological roles of individual cystatins is emerging, e.g., a mutant of cystatin C is associated with hereditary amyloid angiopathy, leading to brain hemorrhage (*7*, *8*), and a deficiency of cystatin B has been demonstrated in a hereditary form of myoclonus epilepsy (*9*, *10*).

Cystatin A, like other cystatins, inhibits lysosomal cysteine proteinases, e.g., cathepsins B, C, H, L, and S, and also cysteine proteinases from parasites e.g., cruzipain, and some plant proteinases, e.g., papain and actinidin, by forming tight, reversible complexes with the enzymes (*6*, *11*−*14*). The solution structure of cystatin A was recently solved by NMR spectroscopy by two independent groups (*15*, *16*) and was found to have considerable similarities with the structures of chicken cystatin and of cystatin B (stefin B) in complex with papain (*17*−*19*). These structures are all consistent with a model for cystatin inhibition of target proteinases, in which inhibition is due to a wedge-shaped edge of the cystatin being inserted into the active-site cleft of the proteinase. This wedge is composed of several residues from the N-terminal region of the inhibitor, a central hairpin-loop (the "first binding loop") and another hairpin-loop (the "second binding loop") close to the C-terminus. In this manner, a large number of interactions between atoms in the contact areas

[†] This work was supported by Swedish Medical Research Council Grant 4212 (to I.B.) and by grants from the Wellcome Trust (to C.J.C.) and BBSRC (to N.J.H.). J.P.W. is a fellow of the Lister Institute of Preventive Medicine.

* To whom correspondence should be addressed at the Department of Veterinary Medical Chemistry. Tel: +46 18 4714191. Fax: +46 18 550762. E-mail: Ingemar.Bjork@vmk.slu.se.

[‡] Swedish University of Agricultural Sciences.

[§] University of Sheffield.

S0006-2960(98)00026-9 CCC: $15.00
Published on Web 05/02/1998

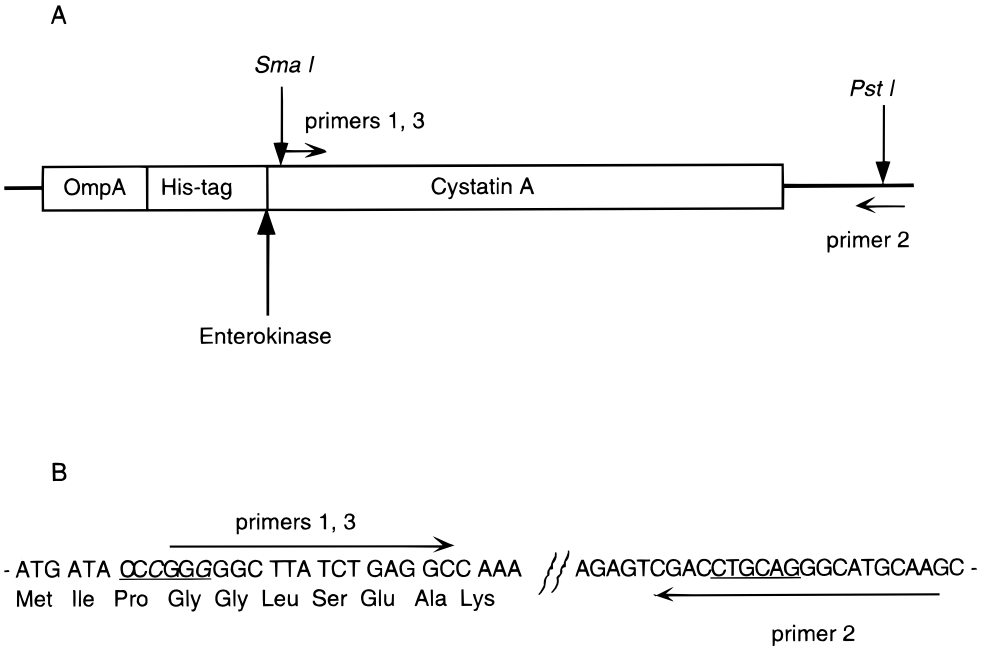

FIGURE 1: (A) Important features of the translated region of the modified expression vector for cystatin A. The OmpA signal peptide targets the fusion protein to the periplasmic space, where processing by a signal peptidase removes the signal peptide. The bold, vertical arrow shows the cleavage site for enterokinase, the enzyme used to release cystatin A, with an authentic N-terminus, from the His-tag affinity handle. The two horizontal arrows represent the upstream (1, 3) and downstream (2) PCR primers used to generate the Gly-4 mutants, as detailed in the Material and Methods section. The DNA fragment excised by digestion with *Sma*I and *Pst*I was replaced with the PCR products containing the Gly-4 mutations. (B) Detailed wiew of the regions in the cystatin A cDNA containing the nucleotides complementary to the PCR primers, represented as arrows. The underlined bases are the cleavage sites for *Sma*I and *Pst*I, separated by 307 bp in the cDNA. The *C* and *G* in codons 3 and 4, replacing A and C in the wild-type cDNA, were introduced to create a unique *Sma*I-site as silent mutations at the same time as the His-tag was engineered.

of the two proteins are formed, explaining the high affinity of the cystatins for their target proteinases, with dissociation constants as low as $\sim 10^{-14}$ M. Data from rapid-kinetic studies of the interaction of cystatins with most proteinases are in agreement with the proposed binding model, indicating a one-step binding mechanism, with close to diffusion-controlled association rate constants and with no evidence for conformational changes (*3*, *13*, *20*−*23*). However, the binding of cystatin C to cathepsin B occurs in two steps, presumably because of the need for the inhibitor to displace the occluding loop that partially covers the active site of this enzyme (*24*).

The contribution to the binding provided by the N-terminal region of the cystatins has been characterized in detail for family II members, e.g., chicken cystatin and human cystatin C, by truncations and modifications of this region, as well as by site-directed mutagenesis of a Gly residue, conserved in all cystatins (*25*−*30*). However, the role played by the shorter N-terminal region of the family I cystatins is less well characterized. Genetically engineered amino acid substitutions and N-terminal truncations of a recombinant cystatin B (stefin B) variant (*31*, *32*), as well as mutations of the conserved glycine and truncations of the N-terminal region of a recombinant cystatin A variant (*33*, *34*), in general have shown decreased affinities of such modified inhibitors for papain. However, the results are somewhat contradictory for the two cystatins, and the magnitudes of the observed effects are uncertain, largely due to difficulties in quantifying the tight interactions involved by equilibrium methods. These difficulties are borne out by the apparent difference of about 4 orders of magnitude between values for the affinity of wild-type cystatin A for papain obtained by equilibrium measurements (*33*) and by a more accurate procedure based on separate measurements of association and dissociation rate constants (*13*). In light of these discrepancies, we have characterized the effects of mutations of the conserved Gly-4 residue in cystatin A on the function of the inhibitor by both equilibrium and kinetic methods. The kinetic methods have allowed us to quantify with confidence some of the very tight interactions involved and also to investigate the mechanism responsible for the decreased affinities caused by the mutations. In addition to papain, we have also studied the inhibition of the more relevant physiological target enzymes, cathepsins B and L, for which the importance of the N-terminal region of cystatin A has not been investigated. We have also characterized the consequences of the mutation for the structures of selected mutants by circular dichroism and NMR.

MATERIALS AND METHODS

Construction of Expression Vectors for Cystatin A Gly-4 Mutants. The previously constructed cystatin A expression vector, containing the cystatin A coding sequence preceded by the leader peptide for OmpA (*13*), was engineered to include a sequence coding for a histidine-tag followed by the recognition site (DDDDK) for the endopeptidase enterokinase, immediately before the first codon of cystatin A (Figure 1). At the same time, a unique restriction site (*Sma*I and *Xma*I) was introduced by mutation of A to C and C to G in positions 9 and 12, respectively, of the cystatin A cDNA, i.e., in the codons for Pro 3 and Gly 4 (Figure 1). These replacements did not affect the amino acid sequence of the translated protein.

For generation of the mutants, G4S-, G4R-, G4E- and G4W-cystatin A,[1] two PCR primers were designed (Figure 1). The upstream primer (5′-*A*/*G*/*T A*/*C*/*G* GGGCTTATCT-GAGGC) was complementary with bases 10−26 in the coding region of cystatin A, although with the first two bases degenerate. The downstream primer (5′-TTGCATGC*CT-GCAG*GTCG) was complementary to a portion in the plasmid beyond the stop codon and included a *Pst*I site. For the G4A cystatin A mutant, a different upstream primer was made (5′-G*CT*GGCTTATCTGAGGC), also annealing from base 10 to 26, but with the second and third bases mismatching (Figure 1).

The expression vector was digested with *Sma*I and *Pst*I, and the resulting fragments, 4303 and 307 bp long, were separated and purified. The short fragment, containing most of the cystatin A coding sequence, was the template for PCR reactions with the primers described above. The products of the reactions were cleaved with *Pst*I and purified. The resulting fragments, blunt-ended upstream and *Pst*I-restricted downstream, were then ligated into the vector that had been cleaved with *Sma*I and *Pst*I. Competent *Escherichia coli* strain MC 1061 was transformed, and individual clones were collected and sequenced to verify that the correct constructs were obtained.

Expression and Purification of Cystatin A Gly-4 Mutants. Expression of both wild-type cystatin A and the Gly-4 mutants was essentially as in ref *13*, i.e., the bacteria were grown at 30 °C, expression was induced at 42 °C, and the content of the periplasmic space was extracted by cold osmotic shock. The expressed proteins were purified by virtue of the attached His-tag. Concentrated buffer was added to the periplasmic extract to give 20 mM Tris-HCl, 500 mM NaCl and 5 mM imidazole, pH 8.0, and the sample was applied to a Ni^{2+} chelate column (Novagen, Inc., Madison, WI) equilibrated with the same buffer. The column was washed with 20 mM Tris-HCl, 500 mM NaCl, and 75 mM imidazole, pH 8.0, and the bound protein was then eluted by increasing the imidazole concentration to 500 mM.

The eluted His-tagged protein was dialyzed against 70 mM Tris-HCl and 2 mM $CaCl_2$, pH 7.4, and incubated with enterokinase (Biozyme, Blaenavon, Great Britain) at a weight ratio of 1:1000 for 16−18 h at 37 °C, which normally resulted in >90% cleavage of the fusion protein. After inactivation of the enterokinase by addition of tosyl phenylalanyl chloromethyl ketone to a concentration of 10 μM, the solution was reapplied to the Ni^{2+} column to remove uncleaved fusion protein and released His-tag. The flow-through fraction was dialyzed against 50 mM Tris-HCl, 100 mM NaCl, 0.1 mM EDTA, pH 7.4.

Enzymes. The purification, properties and storage of papain (EC 3.4.22.2) have been reported elsewhere (*29*, *35*). Cathepsin L (EC 3.4.22.15) from sheep liver (*36*), was a generous gift from Dr. R. W. Mason, Alfred I. du Pont Institute, Wilmington, DE. Human cathepsin B (EC 3.4.22.1) from liver was purchased from Calbiochem (San Diego, CA). The enzymes were activated with 0.5−1 mM dithiothreitol in the reaction buffer (see below) for 5 min at 25 °C before measurements.

Circular Dichroism. Circular dichroism spectra were measured at room temperature (22 ± 2 °C) in a Jasco J-41A spectropolarimeter (Japan Spectroscopic Co., Tokyo, Japan). Measurements were done in the far ultraviolet (200−250 nm) region in cells with 0.1 cm path lengths and with protein concentrations between 0.22 and 0.29 g/L. The bandwidth was 2 nm. A mean residue weight of 112, computed from the amino acid sequence (*37*, *38*), was used for all cystatin variants in the calculations of mean-residue ellipticities.

NMR. Samples of G4A- and G4W-cystatin A for NMR analyses were dialyzed against 50 mM potassium phosphate, 50 mM potassium chloride, pH 5.5. The concentrations of G4A- and G4W-cystatin A were ∼3 and ∼1 mM, respectively. All NMR spectra were acquired at 35 °C on a Bruker AMX-500 spectrometer, as described by Martin et al. (*15*, *39*). Data in the TOCSY experiments (*40*) were acquired with a DIPSI-2 spin locking period of 90 ms. In the NOESY experiment (*41*), data were acquired with a mixing time of 150 ms. Wild-type cystatin A data acquisition has been reported elsewhere (*15*, *39*). All data analysis was carried out with the program FELIX (MSI, San Diego, CA).

Modeling. The mutated cystatin A structures in Figure 2 were created with the program X-PLOR 3.1 (*42*) from the coordinates of Martin et al. (*15*) (PDB code 1DVC) by deleting the ha2 atom of Gly-4 and then using energy minimization to place the atoms of the new side chain, keeping all other atoms in the protein fixed. The coordinates for Figure 4 were constructed by taking the coordinates for the cystatin B-papain complex from Stubbs et al. (*18*) (PDB code 1STF) and adding the tryptophan atoms in position 4, as for the cystatin A structures. However, rather than energy (which is a poor measure of overlap in such a sterically conflicting case), the total number of heavy atom contacts <2 Å was used as the measure of overlap. This parameter was calculated as χ_i was stepped through 360° in 10° steps, and the least overlapping conformation was chosen. Structures were displayed and analyzed with X-PLOR or Rasmol (*43*).

Stoichiometric Titrations. Activated papain, at a constant concentration in the range 2−16 μM, depending on the cystatin A variant titrated, was incubated for 10 min at 25 °C with increasing concentrations of cystatin A variants to give inhibitor:enzyme ratios of 0.2−4.2:1. The residual enzyme activity was determined by diluting the incubation mixture 2-fold with a 600 μM solution of the substrate, N-benzoyl-L-arginine-*p*-nitroanilide, and monitoring the linear rate of product formation by continuous measurement of absorbance at 410 nm for 2−10 min. Substrate hydrolysis never exceeded 5%. The residual activity obtained at each inhibitor concentration was plotted against the molar ratio between inhibitor and enzyme, and the binding stoichiometry was calculated by nonlinear least-squares regression analysis of the data to the equilibrium binding equation (*35*, *44*).

Inhibition Constants. Inhibition constants, K_i, for the interaction of cystatin A mutants with papain, cathepsin L, and cathepsin B were obtained from the equilibrium rates of cleavage of a fluorogenic substrate by the enzyme at

[1] Abbreviations: app, subscript denoting an apparent equilibrium or rate constant measured in the presence of an enzyme substrate; E-64 [*N*−(L-3-*trans*-carboxyoxiran-2-carbonyl)-L-leucyl]-amido-4-guanidobutane; G4A-, G4S-, G4R-, G4E-, and G4W-cystatin A, cystatin A variants in which Gly-4 is replaced with Ala, Ser, Arg, Glu, and Trp, respectively; k_{ass}, bimolecular association rate constant; k_{diss}, dissociation rate constant; K_d, dissociation equilibrium constant; K_i, inhibition constant; k_{obs}, observed pseudo-first-order rate constant; SDS−PAGE, sodium dodecyl sulfate−polyacrylamide gel electrophoresis.

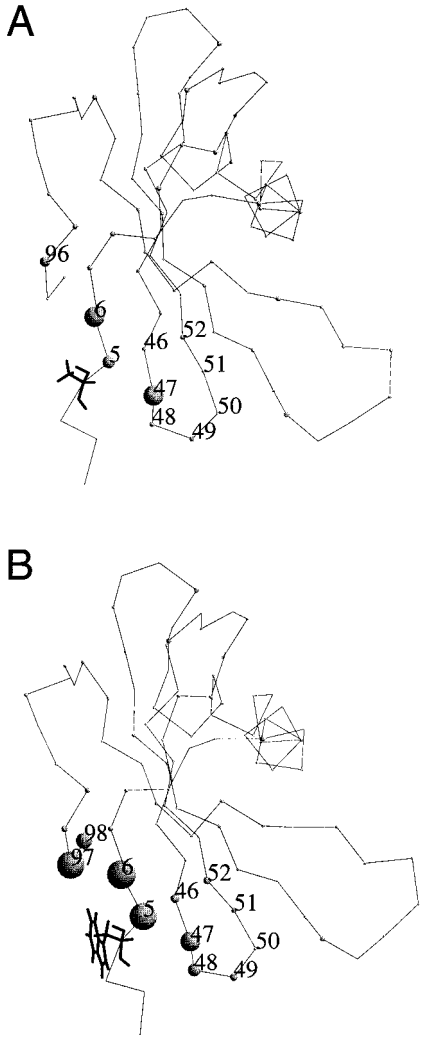

FIGURE 2: Representation of the backbone of wild-type cystatin A, showing the modeled side chain of the mutated residue in position 4 and the chemical shift changes observed by NMR for the G4A (A) and the G4W (B) mutants. Assignments were not made for the disordered residues N-terminal to the mutation. For each other residue, a space-filled sphere is shown at the α-carbon position, the radius of the sphere being proportional to the largest chemical shift change noted in the residue. For scale, the shift changes in panel A were 0.16 ppm for Val-47 and 0.04 ppm for Ala-49 and in panel B were 0.16 ppm for Val-47 and 0.06 ppm for Ala-49.

increasing concentrations of the inhibitor, as described earlier (*29*, *30*). The substrate was carbobenzoxy-L-phenylalanyl-L-arginine 4-methylcoumaryl-7-amide (Peptide Institute, Osaka, Japan) for papain and cathepsin L and carbobenzoxy-L-arginyl-L-arginine 4-methylcoumaryl-7-amide (Peptide Institute) for cathepsin B. The substrate concentration was 10−20 μM; substrate hydrolysis never exceeded 10%. The inhibitor concentration was varied from (0.2 to 1) × $K_{i,app}$ (the apparent inhibition constant) to (2−10) × $K_{i,app}$ and was at least 10-fold higher than that of the enzyme. For slow reactions, the equilibrium rates of substrate hydrolysis were evaluated by nonlinear least-squares regression analyses of the progress curves (*29*). Values for $K_{i,app}$ were obtained by nonlinear regression analyses of plots of the ratio between the inhibited and uninhibited rates of substrate hydrolysis against inhibitor concentration (*45*) and were corrected for substrate competition (*29*, *30*) to give K_i with the use of K_m values reported elsewhere (*29*, *36*, *46*).

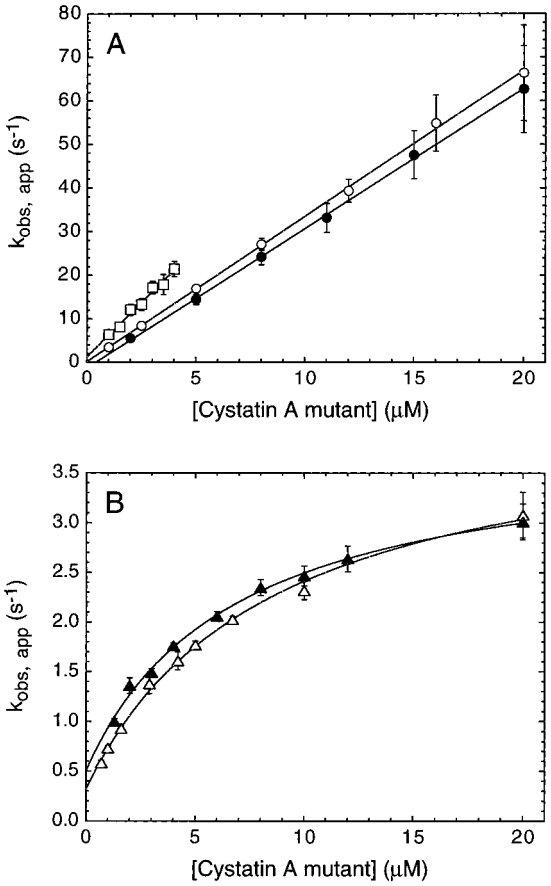

FIGURE 3: Values of $k_{obs,app}$ for the binding of cystatin A Gly-4 mutants to papain as a function of cystatin A concentration. (A) Mutants giving a linear dependence of $k_{obs,app}$ with inhibitor concentration, in accordance with a simple one-step binding mechanism. (○) G4A; (●) G4S; (□) G4W. (B) Mutants giving a hyperbolic dependence of $k_{obs,app}$ with cystatin concentration, consistent with a two-step binding mechanism, as detailed in Scheme 1. (△) G4R; (▲) G4E. The vertical bars represent the standard errors.

Association Kinetics. The rate of binding of cystatin A mutants to papain, cathepsin L, and cathepsin B was evaluated under pseudo-first-order conditions by continuous measurements of the loss of enzyme activity in the presence of a fluorogenic substrate, either in a conventional fluorimeter (F-4000; Hitachi, Tokyo, Japan) or in a stopped-flow apparatus (SX-17MV; Applied Biophysics, Leatherhead, U.K.) essentially as in earlier work (*3*, *29*, *30*). The substrates, their concentrations, and maximal substrate hydrolysis were the same as in the measurements of K_i. The inhibitor concentration was at least 10-fold higher than that of the enzyme. The apparent pseudo-first-order rate constants ($k_{obs,app}$) were obtained by nonlinear least squares regression analyses of the progress curves (*29*). The apparent bimolecular association rate constants, $k_{ass,app}$, derived from plots of $k_{obs,app}$ vs inhibitor concentration, were corrected for substrate competition to give k_{ass} as described above.

Miscellaneous Procedures. SDS−PAGE under reducing conditions was run on 15% gels (*47*). Relative molecular masses and N-terminal sequences were determined as in refs *13* and *20*.

Experimental Conditions and Protein Concentrations. All analyses of inhibitor-proteinase binding were carried out at 25.0 ± 0.2 °C. The buffers used in these analyses were for

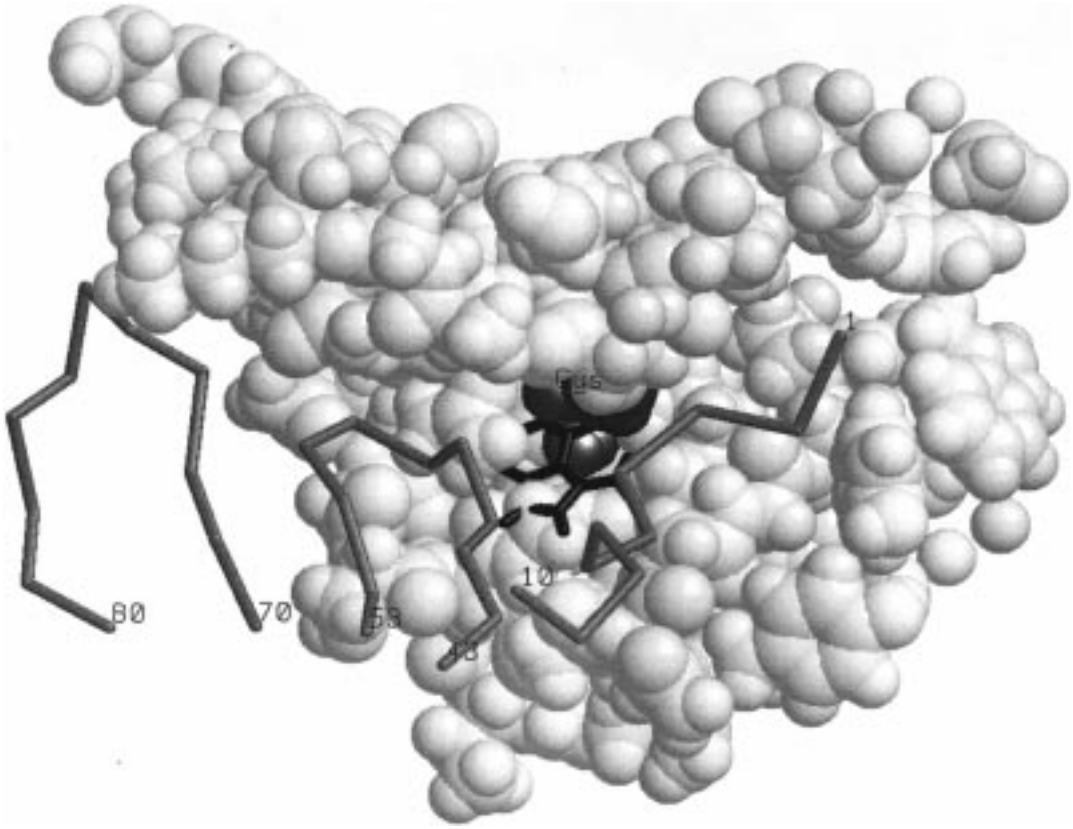

FIGURE 4: Demonstration of the steric incompatibility of a tryptophan substitution at position 4 of cystatin B in the cystatin B−papain complex. The coordinates were obtained as described in Materials and Methods. The region of papain that contacts cystatin B is shown space-filled, with the active-site residue C25 shaded dark gray. The three papain-binding sections of the cystatin B backbone, colored gray, are shown along with the side chain of Trp-4 in black.

papain, 50 mM Tris-HCl, 100 mM NaCl, 0.1 mM EDTA, 1 mM dithiothreitol, and 0.005% (w/v) Brij 35, pH 7.4; for cathepsin L, 100 mM sodium acetate, 1 mM EDTA, 1 mM dithiothreitol, and 0.005% (w/v) Brij 35, pH 5.5; and for cathepsin B, 50 mM Mes, 100 mM NaCl, 0.1 mM EDTA, 0.5 mM dithiothreitol, and 0.1% (w/v) poly(ethylene glycol), pH 6.0.

Concentrations of the cystatin A variants were determined by absorption measurements at 280 nm. The molar absorption coefficient of wild-type cystatin A, 8800 M^{-1} cm^{-1} (*13*), was used for all variants except G4W-cystatin A, for which an absorption coefficient of 14 300 M^{-1} cm^{-1} was calculated from this value by addition of the molar absorption coefficient of one tryptophan residue (*48*). Concentrations of papain were determined by absorption measurements at 280 nm from a molar absorption coefficient of 55 900 M^{-1} cm^{-1} (*35*). The molar concentration of active sites of cathepsin L was determined by titration with E-64 (*36*). The concentration of cathepsin B was provided by the manufacturer.

RESULTS

Expression, Purification, and Properties of Cystatin A Variants. A removable His-tag was inserted into the previously constructed expression vector for cystatin A (*13*) to simplify the purification of both the wild-type inhibitor and the Gly-4 mutants. In particular, affinity chromatography on matrix-linked *S*-(carboxymethyl)papain used previously (*13*) was expected to be inefficient for purification of mutants having appreciably decreased affinities for papain. The degenerate upstream PCR primer that was used to create the Gly-4 cystatin A mutants should have resulted in nine different variants, i.e., G4G-, G4A-, G4S-, G4T-, G4K-, G4R-, G4E-, and G4W-cystatin A, and a stop codon. After partial sequencing of 48 clones, seven of the nine variants were found, but G4A- and G4K-cystatin A were missing. As characterization of the effects of the smallest possible substitution in position 4 was an important part of the study, a specific upstream primer was used to produce the G4A-cystatin A mutant. Wild-type and G4A-, G4S-, G4R-, G4E-, and G4W-cystatin A were expressed and purified in yields from 7 to 12 mg of protein/L of bacterial culture. The inhibitors were >99% pure, as estimated by SDS−PAGE under reducing conditions. N-terminal amino acid sequence analyses of the recombinant cystatins confirmed correct cleavage by enterokinase, producing an authentic N-terminus, and verified that the desired mutations of Gly-4 were present. The relative molecular masses of the variants, as determined by MALDI mass spectroscopy, differed by at most 8 mass units (0.07%) from those expected. Titrations of papain, monitored by the loss of enzyme activity, gave binding stoichiometries of 0.96−1.1:1 for wild-type cystatin A and the G4A and G4S mutants and 0.8−0.9:1 for the G4R, G4E, and G4W mutants. The somewhat lower values for the latter mutants are presumably due to the low affinity of these mutants for papain, which precluded optimal conditions in the determinations of the binding stoichiometries, i.e., a high ratio between the protein concentration and the inhibition constant (*49*). Together, the data show that the expressed and purified inhibitors had the intended mutations and were of correct length and essentially fully active.

Circular Dichroism. Far-UV CD spectra were measured for wild-type cystatin A and all variants except G4W-cystatin A. These spectra all had minima at approximately 215 nm and identical magnitudes within ±5% (not shown). The substitution of Gly-4 thus did not alter the overall conformation of cystatin A sufficiently to perturb the far-UV CD spectrum. G4W-cystatin A was not analyzed, as local interactions between the extra tryptophan side chain and adjacent residues would be expected to substantially affect the far-UV CD spectrum of the protein, even in the absence of a conformational change (*30*, *50*, *51*).

NMR. TOCSY and NOESY spectra were acquired for the G4A and G4W mutants of cystatin A and were of similar high quality to those obtained previously for wild-type cystatin A (*15*, *39*). Resonance assignment was possible by comparison with the wild-type spectra, except for a few residues, less than 10 in each mutant, which showed larger amide shift changes. These residues were assigned by standard sequential assignment methods. A complete table of resonance assignments is available on request.

The largest chemical shift changes within each residue for the two mutants are shown in Figure 2. For guidance, the positions of the side chains of the mutated residues are also shown, as obtained by modeling onto the fixed mean conformation of wild-type cystatin A determined previously (*15*). Apart from a few regions that are discussed further below (see Discussion), the chemical shift changes observed between the mutants and wild-type cystatin A were in general very small, <0.03 ppm.

The NOESY spectra for the mutants were closely superimposable on that of the wild-type, taking into account the shift changes discussed above. The spectra were analyzed in greater detail for the first binding loop by comparing intensities of well resolved peaks in the spectra of the three proteins. Approximately 25 cross-peaks involving residues in the N-terminal region or the first binding loop were examined within each mutant, and no changes in intensity of greater than a factor of approximately 2 were noted. Given the strong dependence of NOESY cross-peak intensity on distance, this difference corresponds to a maximum change in interproton distances of approximately 15%. No nonsequential NOEs to the tryptophan side chain in G4W-cystatin A were observed, indicating that this side chain is in a disordered state.

Inhibition Constants. Dissociation equilibrium constants, K_d, for the binding of the Gly-4 cystatin A mutants to papain and cathepsins L and B were determined as inhibition constants, K_i, by measurements of the decrease caused by the inhibitor of the equilibrium rates of cleavage of a fluorogenic substrate by the proteinase (Table 1). The low affinity for cathepsin B of the variants having substituents with bulky side chains, i.e., G4R-, G4E-, and G4W-cystatin A, only allowed estimations of the lower limits for the K_i of these interactions (Table 1).

Binding Kinetics. Values of k_{ass} for the reactions between the Gly-4 mutants and the cysteine proteinases were determined by continuously monitoring the loss of enzyme activity in the presence of a fluorogenic substrate. Interactions with papain were studied in a stopped-flow instrument with inhibitor concentrations generally ranging from ≤ 1 to 20 μM. However, instrument limitations narrowed the accessible range to 0.5−4 μM for G4W-cystatin A, due to the weak affinity of this mutant for papain. $k_{obs,app}$ for the reaction with papain showed a linear dependence on inhibitor concentration, within the range covered, for the G4A-, G4S-, and G4W-cystatin A mutants (Figure 3A). This behavior is compatible with a single-step binding reaction, as shown previously for the binding of wild-type cystatin A to papain (*13*). The slopes of the plots gave k_{ass} after correction for substrate competition. The dissociation rate constants, k_{diss}, were undeterminable for the G4A and G4S mutants, as the intercepts on the ordinate were indistinguishable from zero, and were instead calculated from K_i and k_{ass} (Table 1). However, a value for k_{diss} could be obtained from the intercept for the G4W cystatin A mutant and was close to that calculated from K_i and k_{ass} (Table 1).

In contrast to the linear behavior observed for the smaller mutants and the G4W mutant, the concentration dependence of $k_{obs,app}$ for the reaction of the G4R- and G4E-cystatin A mutants with papain was hyperbolic (Figure 3B), indicating a two-step binding mechanism. The simplest such mechanism that fits the data can be described as the formation of an initial, weak complex (EI) between enzyme (E) and inhibitor (I) in a rapid equilibrium and with an apparent dissociation constant, $K_{1,app}$, followed by a reversible conformational change with rate constants k_{+2} and k_{-2}, giving the final, stable complex (EI*) (*49*), as shown in Scheme 1.

Scheme 1

$$E + I \overset{K_{1,app}}{\rightleftharpoons} EI \underset{k_{-2}}{\overset{k_{+2}}{\rightleftharpoons}} EI^*$$

$K_{1,app}$, k_{+2}, and k_{-2} were obtained by nonlinear least-squares regression analyses of the data to the equation for this mechanism, $k_{obs,app} = k_{+2}[I]_0/(K_{1,app} + [I]_0) + k_{-2}$ (*49*), where $[I]_0$ is the total concentration of the inhibitor. The values of K_1, corrected for substrate competition, and k_{+2} were $(7.3 \pm 0.9) \times 10^{-6}$ M and (3.9 ± 0.1) s^{-1}, respectively, for the G4R mutant and $(7.1 \pm 1.0) \times 10^{-6}$ M and (3.3 ± 0.1) s^{-1}, respectively, for the G4E mutant. Values of k_{ass} were obtained from the initial slopes, $k_{+2}/K_{1,app}$, of the hyperbolic curves after correction for substrate competition (Table 1). The calculated values for the overall k_{diss} ($k_{diss} = K_i/k_{ass}$) were in good agreement with the fitted values for k_{-2}, which is equal to k_{diss} in the mechanism of Scheme 1 (Table 1).

The kinetics of association of the cystatin A mutants with cathepsin L could only be analyzed for mutants with K_i lower than $\sim 1 \times 10^{-8}$ M, i.e., G4A-, G4S-, and G4W-cystatin A (Table 1), as the amounts of enzyme available precluded measurements at the high concentrations necessary for the weaker-binding mutants. The binding kinetics for the G4A- and G4S-cystatin A mutants were monitored in a conventional fluorimeter, with concentrations of the inhibitors ranging from ~0.5 to 10 nM. Stopped-flow measurements were used to determine the binding kinetics of the G4W mutant to cathepsin L, the concentration of the inhibitor being varied from ~60 to 600 nM. The concentration dependence of $k_{obs,app}$ showed no deviation from linearity for all mutants, the slopes of the plots giving k_{ass} after correction for substrate competition (Table 1). The k_{diss} values obtained from the intercepts on the ordinates were in good agreement with k_{diss} calculated from K_i and k_{ass} (Table 1).

In the case of the interaction between the Gly-4 mutants and cathepsin B, it was only possible to analyze the

Table 1: Values of K_i, k_{ass}, and k_{diss} for the Interaction of Wild-Type Cystatin A and Cystatin A Gly-4 Mutants with Papain, Cathepsin L, and Cathepsin B[a]

enzyme	cystatin A form	K_i (M)	k_{ass} (M^{-1} s^{-1})	k_{diss} (s^{-1})
papain	wild-type	1.8×10^{-13} [b] [1]	3.1×10^6 [1]	5.5×10^{-7} [1]
	G4A	$(1.7 \pm 0.1) \times 10^{-10}$ (13) [900]	$(3.9 \pm 0.05) \times 10^6$ (7) [0.8]	6.6×10^{-4} [c] [1000]
	G4S	$(1.3 \pm 0.1) \times 10^{-9}$ (10) [7000]	$(3.7 \pm 0.05) \times 10^6$ (6) [0.8]	4.8×10^{-3} [c] [9000]
	G4R	$(4.9 \pm 0.3) \times 10^{-7}$ (11) [3×10^6]	5.3×10^5 [d] [6]	0.32 ± 0.06 (9) [6×10^5] 0.26 [c]
	G4E	$(1.3 \pm 0.06) \times 10^{-6}$ (11) [7×10^6]	4.6×10^5 [d] [7]	0.67 ± 0.1 (8) [1×10^6] 0.60 [c]
	G4W	$(5.1 \pm 0.3) \times 10^{-7}$ (11) [3×10^6]	$(5.8 \pm 0.3) \times 10^6$ (7) [0.5]	1.3 ± 0.8 (7) [2×10^6] 3.0 [c]
cathepsin L	wild-type	1.9×10^{-11} [1]	5.2×10^6 [1]	9.9×10^{-5} [c] [1]
	G4A	$(2.2 \pm 0.1) \times 10^{-10}$ (9) [10]	$(8.3 \pm 0.6) \times 10^6$ (9) [0.6]	$(1.6 \pm 0.6) \times 10^{-3}$ (9) [20] 1.8×10^{-3} [c]
	G4S	$(5.7 \pm 0.2) \times 10^{-10}$ (12) [30]	$(7.7 \pm 1.1) \times 10^6$ (12) [0.7]	$(4.7 \pm 0.9) \times 10^{-3}$ (12) [50] 4.3×10^{-3}
	G4R	$(3.3 \pm 0.3) \times 10^{-7}$ (9) [2×10^4]	ND	ND
	G4E	$(1.3 \pm 0.2) \times 10^{-6}$ (7) [7×10^4]	ND	ND
	G4W	$(1.06 \pm 0.03) \times 10^{-8}$ (7) [600]	$(1.3 \pm 0.05) \times 10^7$ (5) [0.4]	0.2 ± 0.1 (5) [2000] 0.14 [c]
cathepsin B	wild-type	9.1×10^{-10} [1]	3.9×10^4 [1]	3.5×10^{-5} [c] [1]
	G4A	$(5.3 \pm 0.4) \times 10^{-6}$ (9) [6000]	$(7.1 \pm 0.5) \times 10^2$ (7) [50]	3.8×10^{-3} [c] [100]
	G4S	$(2.4 \pm 0.1) \times 10^{-5}$ (8) [3×10^4]	$(6.7 \pm 0.4) \times 10^2$ (7) [60]	$(2.4 \pm 0.3) \times 10^{-2}$ (7) [700] 1.6×10^{-2} [c]
	G4R	$>1.3 \times 10^{-4}$ (1) [$>1 \times 10^5$]	ND	ND
	G4E	$>1.1 \times 10^{-4}$ (1) [$>1 \times 10^5$]	ND	ND
	G4W	$\geq 9 \times 10^{-5}$ (3) [$\geq 1 \times 10^5$]	ND	ND

[a] Experimental conditions are described in the Material and Methods. All values for wild-type cystatin A are taken from previous work (*13*) and are shown for comparison. Measured values are given with standard errors and with the number of measurements in parentheses. Calculated values and values obtained previously are given without errors. Relative values, defined as $K_{i,mutant}/K_{i,wild-type}$, $k_{ass,wildtype}/k_{ass,mutant}$ and $k_{diss,mutant}/k_{diss,wild-type}$, are given within square brackets. Relative values of >1 thus indicate changes of K_i, k_{ass} and k_{diss} expected to result in decreased binding affinity. ND, not determined. [b] Calculated from k_{ass} and k_{diss}. [c] Calculated from K_i and k_{ass}. [d] Calculated from the initial slope of the curves in Figure 3B, as described in the Results.

association kinetics for G4A- and G4S-cystatin A, due to the low affinity of the other mutants for cathepsin B (Table 1). For the G4A mutant, the decrease of cathepsin B activity was continuously monitored by conventional fluorimetry, the inhibitor concentrations being varied from 3 to 13 μM, whereas the kinetics of inhibition of the G4S mutant was measured in the stopped-flow fluorimeter with inhibitor concentrations between 25 and 130 μM. k_{obs} showed a linear dependence on the inhibitor concentration for both mutants, the slopes giving k_{ass} (Table 1). A value for k_{diss} could only be determined from the intercept on the ordinate for the G4S mutant and was close to the calculated value (Table 1).

DISCUSSION

Decreased Affinity of the Gly-4 Cystatin A Mutants for Papain, Cathepsin L, and Cathepsin B. These results show that the affinity of Gly-4 mutants of cystatin A for papain in general decreases with increasing size of the side chain of the substituent, in qualitative agreement with a previous report (*33*). However, much larger effects were observed in this work, rendering questionable the simple, quantitative relationship between the size of the side chain in position 4 and the K_i for the mutant proposed previously (*33*). In this study, even the smallest possible substituent, Ala, resulted in about a 1000-fold lower affinity for papain than that of the wild-type (for which K_d is $\sim 1.8 \times 10^{-13}$ M), and substitution to Ser gave a further approximately 8-fold reduction of this affinity. These effects should be compared with those of 10−20-fold reported previously for the same replacements (*33*). Moreover, substitution of Gly-4 by larger or charged substituents, i.e., Arg, Glu, or Trp, resulted in affinity decreases of $\geq 3 \times 10^6$-fold from that of the wild-type, i.e., to a K_i of ~ 1 μM, contrasting much smaller effects of maximally ~250-fold reported previously for comparable

replacements (*33*). These differences are to a large extent due to a much lower K_d for the binding of wild-type cystatin A to papain used in this work. This value was obtained by us in an earlier study by separate measurements of k_{ass} and k_{diss}, a procedure that is much more accurate than equilibrium measurements for very high affinities (*13*). However, also the affinities of the mutants for papain differ between the two investigations, the K_i values obtained in this work being lower than those reported in the previous study, e.g., ~150- and ~40-fold lower for G4A- and G4S-cystatin A, respectively. These discrepancies may be due to the alternative methodology and evaluation procedure used previously (*33*), which is less appropriate for measurements of affinities of the magnitudes involved.

The affinities of the Gly-4 mutants of cystatin A for the physiological target enzymes, cathepsins L and B, not investigated previously, were also found to decrease as the size of the mutant side chain increased. The affinities for cathepsin L in general were comparable with those for papain. However, the affinity decrease was smaller for cathepsin L than for papain, ranging from differences compared with that of the wild-type of approximately 10- and 30-fold for the Ala and Ser mutants, respectively, to differences of $\sim 5 \times 10^4$-fold for the mutants with the larger side chains. This reduced effect may be partly due to a somewhat uncertain value for the affinity of wild-type cystatin A for cathepsin L, $K_i \sim 2 \times 10^{-11}$ M, which could only be obtained by equilibrium measurements, as k_{diss} for the complex could not be determined (*13*). However, the smaller differences most likely also reflect a larger tolerance of cathepsin L than of papain for side chains other than a hydrogen in position 4. Interestingly, the G4W mutant had an anomalously high affinity for cathepsin L, 50-fold higher than that for papain, probably reflecting specific interactions between the indole side chain and the enzyme.

In contrast with the smaller effect seen for cathepsin L compared with papain, the consequences of mutations of Gly-4 in cystatin A were even more deleterious for the binding to cathepsin B than to papain. The decrease in the affinity of the mutants with small side chains, G4A and G4S (the only ones for which values could be obtained), for cathepsin B was ~5000- and ~25000-fold, respectively, K_i being increased to ~5 and ~24 μM, respectively, from ~1 nM for the wild-type. The affinities of G4R-, G4E-, and G4W-cystatin A were indeterminable, but K_i was estimated to be above 100 μM. The large effect of the mutations on the interaction with cathepsin B may be due partially to the "occluding loop", covering a large portion of the active site of the enzyme (*52*) and absent in papain, interfering with the interaction of the new side chains of the mutants with the proteinase.

Evidence That the Decreased Affinity Is Not Caused by a Conformational Change of the Mutants. The observed changes in binding affinity could be due to an altered conformation of cystatin A caused by the mutations or to a change of the interactions between the inhibitor and the enzyme. The circular dichroism spectra gave no evidence for an altered conformation of the cystatin A mutants. Moreover, the very small changes in chemical shift seen in the NMR analyses for the majority of residues provide sensitive evidence that there is no overall conformational change. In G4A-cystatin A, the largest chemical shift changes are observed for Gly-5, Leu-6, and Val-47. These shift changes are small (<0.2 ppm), but indicate that the mutation does have a minor effect on the residues close to it in sequence and also on the first binding loop. In the Trp mutant, the shift changes will have two components: conformational changes in the protein and ring-current effects from the tryptophan aromatic ring system. As the tryptophan side chain appears to be disordered, the ring current effect can very plausibly explain the increased shift changes observed in a number of residues in this mutant, rather than these changes being due to a significantly increased conformational change. This conclusion is supported by the similarity of the pattern of NOEs observed. Although it is difficult to accurately quantify the difference in structure required to effect large changes in K_i, it is clear that the differences in binding affinities between the G4A and G4W mutants are not reflected in the relative size of changes in the structure of the free protein. The circular dichroism and NMR results thus do not support a change in the structure of the inhibitor as being the main cause of the decreased binding energy. Instead, they indicate that the decreased affinities of the G4 cystatin A mutants for proteinases are caused predominantly by the mutant residue interfering with the binding of the N-terminal region of the inhibitor to the proteinase.

Molecular Background to the Decreased Affinity Suggested by Modeling. Computer modeling based on the structure of the cystatin B complex with papain (*18*) provides an indication why the interaction of cystatin A with proteinases is so strongly affected by mutations at the G4 position. The structure of cystatin A, as determined by Martin et al. (*15*), overlays with a backbone root-mean-square deviation of 1.2 Å onto the structure of cystatin B in the complex.[2] Modeling of a tryptophan side chain in position 4 of cystatin B shows that there is severe steric hindrance between the mutated side chain and the proteinase, the majority of the indole group being buried in the papain structure (Figure 4). It is reasonable to assume that this steric hindrance in general should vary with the size of the side chain, which would largely explain the trends in the inhibition data.

Altered Kinetics of Interaction of the Gly-4 Mutants with the Target Enzymes. G4A- and G4S-cystatin A were the only mutants for which the binding kinetics could be analyzed with all enzymes. In the case of papain and cathepsin L, the k_{ass} for the binding of these mutants was unaffected by the mutations, the decrease in affinity being entirely due to an increased k_{diss}. The mutations therefore affect the strength of interactions between cystatin A and papain or cathepsin L that keep the inhibitor and enzyme attached in the complex and not the rate at which these interactions are established. In contrast, in the case of cathepsin B, the mutations affected both k_{ass}, which decreased ~60-fold, and k_{diss}, which increased ~100 and ~700-fold for the G4A and G4S mutants, respectively. This differential effect of the mutations on the rate of association of cystatin A with papain or cathepsin L and with cathepsin B is

[2] An alternative structure of a variant of cystatin A, lacking the N-terminal Met and with Met-65 replaced by Leu, has been determined by Tate et al. (*16*). The structure of this form of the protein does not explain why the mutation at the G4 position affects the chemical shift of Val 47, since it places the N-terminus away from the first binding loop, and this structure therefore will not be considered further here.

analogous to that observed for substitutions in the N-terminal region of cystatin C and for truncation of this region (*25*, *30*). The reduced k_{ass} for the interaction with cathepsin B is consistent with the intact N-terminal region of cystatin A acting in the same manner as that proposed for the corresponding region in cystatin C (*53*), viz., by binding to cathepsin B before the remainder of the inhibitor binding surface. This initial binding facilitates displacement of the "occluding loop" of cathepsin B, allowing full access of the binding surface of the inhibitor to the enzyme reactive site and thus increasing the rate of the reaction.

The hyperbolic concentration dependence of the kinetics of binding of the G4R- and G4E-cystatin A mutants to papain indicate that these residues cannot be accommodated in the complex without conformational changes. In the binding of these mutants, an initial, loose association between inhibitor and proteinase induces a conformational adaptation of one or both moieties, leading to an appreciable increase in binding affinity. The fact that such behavior was not observed for G4W-cystatin A suggests that the conformational changes observed on forming a complex of papain with the G4R and G4E mutants are caused by the charge of the residues replacing Gly-4. It is notable, however, that both the affinity of the initial, weak binding and the rate constant of the induced conformational change are similar for the two mutants, regardless of the opposite charge of the residues introduced. This behavior indicates that highly similar conformational changes are induced in the two cases. Despite the linear concentration dependence of $k_{obs,app}$ for mutants having smaller side chains and for the G4W mutant, it cannot be fully excluded that certain conformational changes are required for complex formation also with these mutants, the kinetics being of such magnitude that these changes escaped detection in our studies.

ACKNOWLEDGMENT

We are grateful to Dr. Robert W. Mason, Alfred I. duPont Institute, Wilmington, DE, for the gift of sheep cathepsin L and to Dr. Åke Engström, Department of Medical and Physiological Chemistry, Uppsala University, Sweden, for determinations of the molecular masses of the cystatin A variants by MALDI mass spectroscopy. We also thank MSI for copies of Felix.

REFERENCES

1. Barrett, A. J., Rawlings, N. D., Davies, M. E., Machleidt, W., Salvesen, G., and Turk, V. (1986) in *Proteinase Inhibitors* (Barrett, A. J., and Salvesen, G., Eds.) pp 515−569, Elsevier, Amsterdam.
2. Freije, J. P., Abrahamson, M., Olafsson, I., Velasco, G., Grubb, A., and Lopez-Otin, C. (1991) *J. Biol. Chem. 266*, 20538−20543.
3. Turk, B., Stoka, V., Björk, I., Boudier, C., Johansson, G., Dolenc, I., Čolic, A., Bieth, J. G., and Turk, V. (1995) *Protein Sci. 4*, 1874−1890.
4. Sloane, B. F. (1990) *Semin. Cancer Biol. 1*, 137−152.
5. North, M. J., Robertson, C. D., and Coombs, G. H. (1990) *Mol. Biochem. Parasitol. 39*, 183−193.
6. Stoka, V., Nycander, M., Lenarčič, B., Labriola, C., Cazzulo, J. J., Björk, I., and Turk, V. (1995) *FEBS Lett. 370*, 101−104.
7. Ghiso, J., Jensson, O., and Frangione, B. (1986) *Proc. Natl. Acad. Sci. U.S.A. 83*, 2974−2978.
8. Palsdottir, A., Abrahamson, M., Thorsteinsson, L., Arnason, A., Olafsson, I., Grubb, A., and Jensson, O. (1988) *Lancet 2*, 603−604.
9. Pennacchio, L. A., Lehesjoki, A. E., Stone, N. E., Willour, V. L., Virtaneva, K., Miao, J. M., D'Amato, E., Ramirez, L., Faham, M., Koskiniemi, M., Warrington, J. A., Norio, R., De la Chapelle, A., Cox, D. R., and Myers, R. M. (1996) *Science 271*, 1731−1734.
10. Lalioti, M. D., Mirotsou, M., Buresi, C., Peitsch, M. C., Rossier, C., Ouazzani, R., Baldy-Moulinier, M., Bottani, A., Malafosse, A., and Antonarakis, S. E. (1997) *Am. J. Hum. Genet. 60*, 342−351.
11. Green, G. D., Kembhavi, A. A., Davies, M. E., and Barrett, A. J. (1984) *Biochem. J. 218*, 939−946.
12. Abrahamson, M., Barrett, A. J., Salvesen, G., and Grubb, A. (1986) *J. Biol. Chem. 261*, 11282−11289.
13. Pol, E., Olsson, S. L., Estrada, S., Prasthofer, T. W., and Björk, I. (1995) *Biochem. J. 311*, 275−282.
14. Leonardi, A., Turk, B., and Turk, V. (1996) *Biol. Chem. Hoppe-Seyler 377*, 319−321.
15. Martin, J. R., Craven, C. J., Jerala, R., Kroon-Žitko, L., Žerovnik, E., Turk, V., and Waltho, J. P. (1995) *J. Mol. Biol. 246*, 331−343.
16. Tate, S., Ushioda, T., Utsunomiya-Tate, N., Shibuya, K., Ohyama, Y., Nakano, Y., Kaji, H., Inagaki, F., Samejima, T., and Kainosho, M. (1995) *Biochemistry 34*, 14637−14648.
17. Bode, W., Engh, R., Musil, D., Thiele, U., Huber, R., Karshikov, A., Brzin, J., Kos, J., and Turk, V. (1988) *EMBO J. 7*, 2593−2599.
18. Stubbs, M. T., Laber, B., Bode, W., Huber, R., Jerala, R., Lenarčič, B., and Turk, V. (1990) *EMBO J. 9*, 1939−1947.
19. Dieckmann, T., Mitschang, L., Hofmann, M., Kos, J., Turk, V., Auerswald, E. A., Jaenicke, R., and Oschkinat, H. (1993) *J. Mol. Biol. 234*, 1048−1059.
20. Björk, I., Alriksson, E., and Ylinenjärvi, K. (1989) *Biochemistry 28*, 1568−1573.
21. Björk, I., and Ylinenjärvi, K. (1990) *Biochemistry 29*, 1770−1776.
22. Lindahl, P., Abrahamson, M., and Björk, I. (1992) *Biochem. J. 281*, 49−55.
23. Turk, B., Čolic, A., Stoka, V., and Turk, V. (1994) *FEBS Lett. 339*, 155−159.
24. Nycander, M., Estrada, S., Mort, J. S., Abrahamson, M., and Björk, I. (1998) *FEBS Lett. 422*, 61−64.
25. Abrahamson, M., Mason, R. W., Hansson, H., Buttle, D. J., Grubb, A., and Ohlsson, K. (1991) *Biochem. J. 273*, 621−626.
26. Machleidt, W., Thiele, U., Laber, B., Assfalg-Machleidt, I., Esterl, A., Wiegand, G., Kos, J., Turk, V., and Bode, W. (1989) *FEBS Lett. 243*, 234−238.
27. Popovič, T., Brzin, J., Ritonja, A., and Turk, V. (1990) *Biol. Chem. Hoppe-Seyler 371*, 575−580.
28. Lindahl, P., Nycander, M., Ylinenjärvi, K., Pol, E., and Björk, I. (1992) *Biochem. J. 286*, 165−171.
29. Björk, I., Pol, E., Raub-Segall, E., Abrahamson, M., Rowan, A. D., and Mort, J. S. (1994) *Biochem. J. 299*, 219−225.
30. Björk, I., Brieditis, I., and Abrahamson, M. (1995) *Biochem. J. 306*, 513−518.
31. Thiele, U., Assfalg-Machleidt, I., Machleidt, W., and Auerswald, E. A. (1990) *Biol. Chem. Hoppe-Seyler 371* (Suppl.), 125−136.
32. Machleidt, W., Thiele, U., Assfalg-Machleidt, I., Forger, D., and Auerswald, E. A. (1991) *Biomed. Biochim. Acta 50*, 613−620.
33. Shibuya, K., Kaji, H., Ohyama, Y., Tate, S., Kainosho, M., Inagaki, F., and Samejima, T. (1995) *J. Biochem. (Tokyo) 118*, 635−642.
34. Shibuya, K., Kaji, H., Itoh, T., Ohyama, Y., Tsujikami, A., Tate, S., Takeda, A., Kumagai, I., Hirao, I., Miura, K., Inagaki, F., and Samejima, T. (1995) *Biochemistry 34*, 12185−12192.
35. Lindahl, P., Alriksson, E., Jörnvall, H., and Björk, I. (1988) *Biochemistry 27*, 5074−5082.
36. Mason, R. W. (1986) *Biochem. J. 240*, 285−288.

37. Kartasova, T., Cornelissen, B. J., Belt, P., and van de Putte, P. (1987) *Nucleic Acids Res. 15*, 5945−5962.
38. Machleidt, W., Borchart, U., Fritz, H., Brzin, J., Ritonja, A., and Turk, V. (1983) *Hoppe-Seyler's Z. Physiol. Chem. 364*, 1481−1486.
39. Martin, J. R., Jerala, R., Kroon-Žitko, L., Žerovnik, E., Turk, V., and Waltho, J. P. (1994) *Eur. J. Biochem. 225*, 1181−1194.
40. Rance, M. (1987) *J. Magn. Reson. 74*, 557−564.
41. Macura, S., Huang, Y., Suter, D., and Ernst, R. R. (1981) *J. Magn. Reson. 43*, 259−281.
42. Brünger, A. T. (1992) in *X-PLOR. A System for X-ray Crystallography and NMR*, Yale University Press, New Haven.
43. Sayle, R. A. and Milner-White, E. J. (1995) *Trends Biochem. Sci. 20*, 374−376.
44. Nordenman, B. and Björk, I. (1978) *Biochemistry 17*, 3339−3344.
45. Butterfield, D. A., and Lee, J. (1994) *Arch. Biochem. Biophys. 310*, 167−171.
46. Hall, A., Abrahamson, M., Grubb, A., Trojnar, J., Kania, P., Kasprzykowska, R., and Kasprzykowski, F. (1992) *J. Enzyme Inhib. 6*, 113−123.
47. Laemmli, U. K. (1970) *Nature 227*, 680−685.
48. Gill, S. C. and von Hippel, P. H. (1989) *Anal. Biochem. 182*, 319−326.
49. Bieth, J. G. (1995) *Methods Enzymol. 248*, 59−84.
50. Holladay, L. A. and Puett, D. (1976) *Biopolymers 15*, 43−59.
51. Holladay, L. A., Rivier, J., and Puett, D. (1977) *Biochemistry 16*, 4895−4900.
52. Musil, D., Zučič, D., Turk, D., Engh, R. A., Mayr, I., Huber, R., Popovič, T., Turk, V., Towatari, T., Katunuma, N., and Bode, W. (1991) *EMBO J. 10*, 2321−2330.
53. Björk, I., Brieditis, I., Raub-Segall, E., Pol, E., Håkansson, K., and Abrahamson, M. (1996) *Biochemistry 35*, 10720−10726.

BI980026R